COMPLEX NONSEPARABLE OVERSAMPLED LAPPED TRANSFORM FOR SPARSE REPRESENTATION OF MILLIMETER WAVE RADAR IMAGE

Satoshi NAGAYAMA[1], *Shogo MURAMATSU*[2*], *Hiroyoshi YAMADA*[2] *and Yuuichi SUGIYAMA*[3]

[1]Graduate School of Science and Technology, Niigata Univ., Japan
[2]Faculty of Engineering, Niigata Univ., Japan
[3]FUJITSU TEN LIMITED, Japan

ABSTRACT

This work generalizes an existing framework of nonseparable oversampled lapped transforms (NSOLTs) to effectively represent complex-valued images. The original NSOLTs are lattice-structure-based redundant transforms, which satisfy the linear-phase, compact-supported and real-valued property. The lattice structure is able to constitute a Parseval tight frame with rational redundancy and to generate a dictionary with directional atomic images. In this study, a generalized structure of NSOLTs is proposed to cover complex-valued atomic images. The novel transform is referred to as a complex NSOLT (ℂNSOLT). The effectiveness of the structure is verified by evaluating the sparse approximation performance using the iterative hard thresholding (IHT) algorithm for a millimeter wave radar image.

***Index Terms*—** Complex dictionary, Parseval tight frame, NSOLT, Millimeter wave radar, Sparse approximation

1. INTRODUCTION

Oversampled filterbanks, or redundant transforms, have found a lot of image processing applications such as denoising, deblurring, super-resolution, inpainting and compressive sensing [1–6]. In most of such applications, filterbanks are explicitly or implicitly used to sparsely represent a given image as a linear-combination of image prototypes, which are referred to as atomic images. Thus, the selection of a set of atomic images is a quite important task to determine the generative model of a set of target images.

In the article [7], a framework of nonseparable oversampled lapped transforms (NSOLTs) is proposed. NSOLTs allow us to achieve an overcomplete analysis-synthesis system with nonseparable, symmetric, overlapped and compact-supported atomic images. NSOLTs are based on lattice structures, where the redundancy is flexibly controlled by the number of channels and downsampling ratio. Even though the atomic images are nonseparable, the analysis and synthesis process can be factorized into separate dimensional operations in the polyphase domain [8]. As well, the structures are capable of constructing Parseval tight frames, and an example-based design method is available [9, 10].

The effectiveness of NSOLTs was verified by examining design samples and evaluating their sparse approximation performance using the iterative hard thresholding (IHT) algorithm for natural images and MRI volumetric data [7]. The existing framework, however, considers only the real-valued images as target data. Thus, there remains a room to improve the performance for complex-valued images, such as radar, sonar, electromagnetics, and accoustic ones [11, 12].

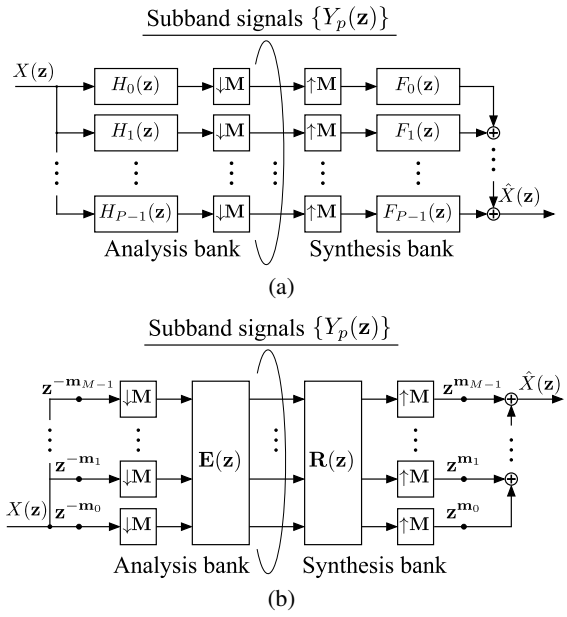

Fig. 1. (a) Parallel structure of a P-channel filter banks with downsampling factor $\mathbf{M}$ and (b) the polyphase matrix representation, where $\{H_p(\mathbf{z})\}$ and $\{F_p(\mathbf{z})\}$ are analysis and synthesis filters, respectively.

Fig. 1 (a) shows a parallel structure of P-channel multidimensional nonseparable filterbanks. The system consists of an analysis and synthesis bank, where $\mathbf{z} \in \mathbb{C}^D$ denotes a $D \times 1$ complex variable vector in the D-dimensional z-transform domain, $H_p(\mathbf{z})$ and $F_p(\mathbf{z})$ are the transfer functions of the p-th analysis and synthesis filter, respectively. In the followings, we consider only the two-dimensional (2-D) separable decimation case, i.e., $D = 2$. The symbol $\downarrow \mathbf{M}$ and $\uparrow \mathbf{M}$ are the downsampler and upsampler with factor $\mathbf{M} = \mathrm{diag}(M_\mathrm{v}, M_\mathrm{h}) \in \mathbb{Z}^{2\times 2}$, respectively [7, 13]. The sampling ratio of each channel is given by $M = |\det(\mathbf{M})| = |M_\mathrm{v} M_\mathrm{h}|$, and the redundancy of subband signals is calculated as $R = P/M$.

Dual-tree complex wavelet transform (DT-ℂWT) is a good candidate for sparsely representing complex-valued images [14]. DT-ℂWT has nearly shift invariant and directionally selective. As well, the atomic images are nonseparable and compact-supported. However, due to its hierarchical tree structure with two-channel filter-

*This work was supported by JSPS KAKENHI (JP26420347, JP17H03261).

banks, we have to give up either of the tight or symmetric property. The redundancy is also restricted to be $2D$ for D-dimensional signals, i.e., an integer more than two.

The original NSOLTs are able to simultaneously satisfy both of the tight and symmetric property. As well, the redundancy can be rational, and even be less than two [9]. In this paper, we propose a novel framework for constructing redundant complex-valued transforms by generalizing the existing real-valued NSOLT structure. We refer to the novel NSOLT as complex NSOLT ($\mathbb{C}$NSOLT). In order to verify the significance, we evaluate the sparse approximation performance by using IHT for a millimeter wave radar image and compare the result with that of the original real-valued NSOLT.

2. REVIEW OF SPARSE APPROXIMATION

In this section, we review a formulation of sparse approximation problem for complex-valued images, and then introduce IHT algorithm as a heuristic solver for the problem.

2.1. Problem Formulation

Let $\mathbf{x} \in \mathbb{C}^N$ be a vectorized complex image with N pixels, where we can adopt simple column stacking of entire image. Then, a matrix $\mathbf{D} \in \mathbb{C}^{N\times L}$ can be used to represent $\mathbf{x}$ as

$$\mathbf{x} = \mathbf{D}\mathbf{y}, \tag{1}$$

with a coefficient vector $\mathbf{y} \in \mathbb{C}^L$, where $N \leq L$.

Sparse approximation is a problem of finding a sparse coefficient vector $\hat{\mathbf{y}} \in \mathbb{C}^L$. This problem is formulated as

$$\hat{\mathbf{y}} = \arg\min_{\mathbf{y}} \|\mathbf{x} - \mathbf{D}\mathbf{y}\|_2^2 \text{ s.t. } \|\mathbf{y}\|_0 \leq K, \tag{2}$$

where $\|\cdot\|_0$ denotes the number of nonzero elements and $K \ll N$. The above problem is NP-hard, and we need to adopt a suboptimal approach. Orthogonal matching pursuit (OMP) and IHT are good candidates for the solvers.

Note here that the performance of the sparse approximation is strongly dependent not only on the adopted solver but also the adopted dictionary $\mathbf{D}$. A dictionary can also be used in sparsity-aware image restoration techniques [4]. The sparse approximation performance is a good indicator for the image restoration performance.

2.2. Iterative Hard Thresholding (IHT)

A synthesis bank shown in right hand side of Fig. 1 is a discrete linear operator for subband signals $\{Y_p(\mathbf{z})\}$ and can be expressed as a matrix by isomorphism, where the matrix has exactly the same role as the dictionary $\mathbf{D}$ in (1) [7].

Because of the overlapping property of filters, i.e., atomic images in the dictionary $\mathbf{D}$, the matrix size becomes huge and the application to sparse approximation requires a solver available for large data. IHT is a suitable solver in such a situation since it requires no inverse operator but, instead, processes with an adjoint operator [15].

Algorithm 1 shows the IHT algorithm, where $\mathbf{D}^H$ denotes the Hermitian transposition of $\mathbf{D}$, μ is a real number close to but less than unity and $\epsilon > 0$. $\mathcal{H}_K(\cdot)$ is the hard thresholding operation defined by

$$\mathcal{H}_K(\mathbf{v}) = \mathbf{v} \odot \mathbf{1}_{(|\mathbf{v}|>\lambda_K)}, \tag{3}$$

where $\mathbf{1}_{(|\mathbf{v}|>\lambda_K)}$ denotes a function that replaces K absolute values greater than λ_K to 1 and the others to 0, where λ_K is the K-th largest absolute value among elements in $\mathbf{v}$. Symbol $\odot$ denotes element-wise product, i.e., Hadamard product [15].

Algorithm 1 Iterative hard thresholding (IHT) algorithm

Data: Source $\mathbf{x} \in \mathbb{C}^N$
Result: Approximation $\hat{\mathbf{x}} \in \mathbb{C}^N$
{Initialization}
$t \leftarrow 0$
$\mathbf{y}^{(0)} \leftarrow \mathbf{D}^H\mathbf{x}$
{Main iteration to heuristically find $\mathbf{y}$ that minimizes $\|\mathbf{x} - \mathbf{D}\mathbf{y}\|_2^2$ s.t. $\|\mathbf{y}\|_0 \leq K$}
repeat
  $t \leftarrow t + 1$
  $\mathbf{y}^{(t)} \leftarrow \mathcal{H}_K\left(\mathbf{y}^{(t-1)} + \mu\mathbf{D}^H\left(\mathbf{x} - \mathbf{D}\mathbf{y}^{(t-1)}\right)\right)$
until $\|\mathbf{y}^{(t)} - \mathbf{y}^{(t-1)}\|_2^2/\|\mathbf{y}^{(t)}\|_2^2 < \epsilon$
$\hat{\mathbf{x}} \leftarrow \mathbf{D}\mathbf{y}^{(t)}$

3. COMPLEX NSOLT ($\mathbb{C}$NSOLT)

The dictionary $\mathbf{D}$ determines a generative model of a given set of images and influences the sparse approximation performance in (2). In this section, let us propose $\mathbb{C}$NSOLT as a dictionary $\mathbf{D}$ by generalizing the existing real-valued NSOLT ($\mathbb{R}$NSOLT) framework.

3.1. Parallel Structure and Polyphase Representation

The analysis bank $\{H_p(\mathbf{z})\}_{p=0}^{P-1}$ and synthesis bank $\{F_p(\mathbf{z})\}_{p=0}^{P-1}$ shown in Fig. 1 are respectively represented by

$$\mathbf{h}(\mathbf{z}) = \begin{pmatrix} H_0(\mathbf{z}), & H_1(\mathbf{z}), & \cdots, & H_{P-1}(\mathbf{z}) \end{pmatrix}^T = \mathbf{E}(\mathbf{z}^{\mathbf{M}})\mathbf{d}(\mathbf{z}),$$
$$\mathbf{f}^T(\mathbf{z}) = \begin{pmatrix} F_0(\mathbf{z}), & F_1(\mathbf{z}), & \cdots, & F_{P-1}(\mathbf{z}) \end{pmatrix} = \mathbf{d}^T(\mathbf{z}^{-\mathbf{I}})\mathbf{R}(\mathbf{z}^{\mathbf{M}})$$

in terms of polynomial matrices $\mathbf{E}(\mathbf{z})$ and $\mathbf{R}(\mathbf{z})$, where the superscript 'T' denotes the transposition, '$\mathbf{I}$' is the identity matrix and $\mathbf{d}(\mathbf{z})$ shows a 2-D delay chain vector of size $M \times 1$, i.e., $\mathbf{d}_{\mathbf{M}}(\mathbf{z}) = \left(\mathbf{z}^{-\mathbf{m}_0}, \mathbf{z}^{-\mathbf{m}_1}, \cdots, \mathbf{z}^{-\mathbf{m}_{M-1}}\right)^T$. $\mathbf{E}(\mathbf{z})$ and $\mathbf{R}(\mathbf{z})$ are of size $P \times M$ and $M \times P$, respectively.

3.1.1. Linear-Phase (Symmetric) Condition

Suppose that all filters $\{H_p(\mathbf{z})\}_{p=0}^{P-1}$ and $\{F_p(\mathbf{z})\}_{p=0}^{P-1}$ are of size $L_{\mathrm{v}} \times L_{\mathrm{h}} = (N_{\mathrm{v}}+1)M_{\mathrm{v}} \times (N_{\mathrm{h}}+1)M_{\mathrm{h}}$. The polyphase order $\bar{\mathbf{n}}$ is given by $\bar{\mathbf{n}} = (N_{\mathrm{v}}, N_{\mathrm{h}})^T$, and the linear-phase (LP) conditions for the complex-valued analysis and synthesis bank are represented as

$$\mathbf{E}(\mathbf{z}) = \mathbf{z}^{-\bar{\mathbf{n}}}\mathbf{\Gamma}_P\mathbf{E}_*(\mathbf{z}^{-\mathbf{I}})\mathbf{J}_M, \tag{4}$$
$$\mathbf{R}(\mathbf{z}) = \mathbf{z}^{-\bar{\mathbf{n}}}\mathbf{J}_M\mathbf{R}_*(\mathbf{z}^{-\mathbf{I}})\mathbf{\Gamma}_P^*, \tag{5}$$

respectively, where $\mathbf{J}_M$ is the $M \times M$ counter identity matrix, and $\mathbf{\Gamma}_P$ is a $P \times P$ diagonal matrix with diagonal elements $\gamma_p \in \{\gamma \in \mathbb{C} | \ |\gamma| = 1\}$, which determines the symmetry of filters. The subscript asterisk means the complex conjugate only for the coefficients.

3.1.2. Perfect Reconstruction and Paraunitary Condition

The perfect reconstruction (PR) condition is sufficiently represented by $\mathbf{R}(\mathbf{z})\mathbf{E}(\mathbf{z}) = \mathbf{z}^{-\bar{\mathbf{n}}}\mathbf{I}_M$ in terms of the polyphase matrices, where $\mathbf{I}_M$ is the $M \times M$ identity matrix. If the condition

$$\mathbf{E}_*^T(\mathbf{z}^{-\mathbf{I}})\mathbf{E}(\mathbf{z}) = \mathbf{I}_M, \tag{6}$$

is satisfied, then $\mathbf{E}(\mathbf{z})$ is said to be paraunitary (PU). Furthermore, a PU synthesis bank is obtained by the para-conjugation of $\mathbf{E}(\mathbf{z})$ as

$$\mathbf{R}(\mathbf{z}) = \mathbf{z}^{-\bar{\mathbf{n}}}\mathbf{E}_*^T(\mathbf{z}^{-\mathbf{I}}). \tag{7}$$

A pair of such analysis and synthesis bank not only satisfy the PR condition, but also adjoin to each other. In other words, a dictionary $\mathbf{D}$ determined by a PU synthesis bank $\mathbf{R}(\mathbf{z})$ constitutes a tight frame.

3.2. Product Form of Complex-valued LPPR Filterbanks

A complex-valued P-channel LPPR FIR analysis bank is obtained by a cascade construction of propagation matrices $\{\mathbf{G}_{n_d}^{\{d\}}(z_d)\}$ as

$$\mathbf{E}(\mathbf{z}) = \mathbf{\Phi} \prod_{d\in\{\mathrm{v},\mathrm{h}\}} \left(\prod_{k=1}^{K_d} \mathbf{G}_k^{\{d\}}(z_d) \right) \cdot \mathbf{E}_0(\mathbf{z}), \tag{8}$$

where $\mathbf{E}_0(\mathbf{z})$ is a $P \times M$ initial matrix of polyphase order $\bar{\mathbf{n}}_{\mathrm{I}} = (N_{\mathrm{Iv}}, N_{\mathrm{Ih}})^T$, $\mathbf{\Phi}$ is a $P \times P$ diagonal matrix satisfying $\mathbf{\Phi}^2 = \mathbf{\Gamma}_P^*$, where the superscript asterisk denotes the complex conjugation, and $\{\mathbf{G}_k^{\{d\}}(z_d)\}$ is a $P\times P$ propagation matrices of which the polyphase order in the d-th dimension is $N_{\mathrm{G}d} \in \mathbb{N}$ and the others are zero.

The condition on $\mathbf{G}_k^{\{d\}}(z_d)$ for $\mathbf{E}(\mathbf{z})$ to satisfy both of the LP and PR property is summarized in the following theorems:

Theorem 1 *If each $\mathbf{G}_k^{\{d\}}(z_d)$ is FIR invertible, i.e., the determinant is a monomial in z_d, and satisfies*

$$\mathbf{G}_k^{\{d\}}(z_d) = z_d^{-N_{\mathrm{G,d}}} \mathbf{G}_{*,k}^{\{d\}}(z_d^{-1}),\ d \in \{\mathrm{v},\mathrm{h}\} \tag{9}$$

then $\mathbf{E}(\mathbf{z})$ corresponds to an LPPR filterbank with all filters of size $L_{\mathrm{v}} \times L_{\mathrm{h}} = (K_{\mathrm{v}}N_{\mathrm{Gv}} + N_{\mathrm{Iv}} + 1)M_{\mathrm{v}} \times (K_{\mathrm{h}}N_{\mathrm{Gh}} + N_{\mathrm{Ih}} + 1)M_{\mathrm{h}}$.

Theorem 2 *If $\mathbf{G}_{k_d}^{\{d\}}(z_d)$ is invertible and satisfies* (9) *with $N_{\mathrm{G},d} = 1$, then P must be even.*

We here omit to show the proofs for the above theorems. It can be proved that the product $N_{\mathrm{G},d}P$ must be even. In the case of $N_{\mathrm{G},d} = 1$, Theorem 1 reduced to one of the critically-sampled case [16].

In summary, a complex-valued P-channel LPPR filterbanks in the form (8) are categorized into the following two types according to the number of channels P:

1. Type-I: P is even and $N_{\mathrm{G},d} = 1$ for $d \in \{\mathrm{v},\mathrm{h}\}$,
2. Type-II: P is odd and $N_{\mathrm{G},d} = 2$ for $d \in \{\mathrm{v},\mathrm{h}\}$.

Different from the real-valued case, the symmetry is not restricted to $\gamma_p = \pm 1$ and the condition is relaxed.

3.3. Lattice Structure of ℂNSOLT

Let us propose a construction of propagation matrix $\{\mathbf{G}_{n_d}^{\{d\}}(z_d)\}$ to yield a lattice structure of a complex version of NSOLTs. In the followings, we only consider the Type-I case. Fig.2 shows a proposed lattice structure of an analysis bank of Type-I ℂNSOLT. The polyphase matrix $\mathbf{E}(\mathbf{z})$ of Type-I ℂNSOLT is given by

$$\mathbf{E}(\mathbf{z}) = \mathbf{\Phi} \left(\prod_{k=1}^{K_{\mathrm{v}}} \mathbf{G}_k^{\{\mathrm{v}\}}(z_{\mathrm{v}}) \right) \left(\prod_{k=1}^{K_{\mathrm{h}}} \mathbf{G}_k^{\{\mathrm{h}\}}(z_{\mathrm{h}}) \right) \mathbf{E}_0(\mathbf{z}), \tag{10}$$

where

$$\mathbf{\Phi} = \mathrm{diag}\left(e^{j\phi_0}, e^{j\phi_1}, \cdots, e^{j\phi_{P-1}}\right),$$
$$\mathbf{G}_k^{\{d\}}(z_d) = \mathbf{V}_k^{\{d\}} \mathbf{Q}_k^{\{d\}}(z_d),$$
$$\mathbf{V}_k^{\{d\}} = \begin{pmatrix} \mathbf{W}_k^{\{d\}} & \mathbf{O} \\ \mathbf{O} & \mathbf{U}_k^{\{d\}} \end{pmatrix},$$
$$\mathbf{Q}_k^{\{d\}}(z_d) = \frac{1}{2} \hat{\mathbf{B}}_k^{\{d\}} \mathbf{\Lambda}_P(z_d) \hat{\mathbf{B}}_k^{\{d\}H},$$
$$\hat{\mathbf{B}}_k^{\{d\}} = \begin{pmatrix} \hat{\mathbf{C}}_k^{\{d\}} & \hat{\mathbf{C}}_k^{\{d\}*} \\ \hat{\mathbf{S}}_k^{\{d\}} & \hat{\mathbf{S}}_k^{\{d\}*} \end{pmatrix},$$
$$\hat{\mathbf{C}}_k^{\{d\}} = \begin{cases} \mathrm{diag}\left(\hat{\mathbf{c}}_{k,0}^{\{d\}}, \hat{\mathbf{c}}_{k,1}^{\{d\}}, \cdots, \hat{\mathbf{c}}_{k,\lfloor \frac{P}{4} \rfloor - 1}^{\{d\}}\right), & \lfloor \frac{P}{2} \rfloor \text{: even} \\ \mathrm{diag}\left(\hat{\mathbf{c}}_{k,0}^{\{d\}}, \hat{\mathbf{c}}_{k,1}^{\{d\}}, \cdots, \hat{\mathbf{c}}_{k,\lfloor \frac{P}{4} \rfloor - 1}^{\{d\}}, 1\right), & \lfloor \frac{P}{2} \rfloor \text{: odd} \end{cases},$$
$$\hat{\mathbf{S}}_k^{\{d\}} = \begin{cases} \mathrm{diag}\left(\hat{\mathbf{s}}_{k,0}^{\{d\}}, \hat{\mathbf{s}}_{k,1}^{\{d\}}, \cdots, \hat{\mathbf{s}}_{k,\lfloor \frac{P}{4} \rfloor - 1}^{\{d\}}\right), & \lfloor \frac{P}{2} \rfloor \text{: even} \\ \mathrm{diag}\left(\hat{\mathbf{s}}_{k,0}^{\{d\}}, \hat{\mathbf{s}}_{k,1}^{\{d\}}, \cdots, \hat{\mathbf{s}}_{k,\lfloor \frac{P}{4} \rfloor - 1}^{\{d\}}, j\right), & \lfloor \frac{P}{2} \rfloor \text{: odd} \end{cases},$$
$$\hat{\mathbf{c}}_{k,p}^{\{d\}} = \begin{pmatrix} -j\cos\theta_{k,p}^{\{d\}} & -j\sin\theta_{k,p}^{\{d\}} \\ \cos\theta_{k,p}^{\{d\}} & -\sin\theta_{k,p}^{\{d\}} \end{pmatrix} \in \mathbb{C}^{2\times 2},$$
$$\hat{\mathbf{s}}_{k,p}^{\{d\}} = \begin{pmatrix} \sin\theta_{k,p}^{\{d\}} & \cos\theta_{k,p}^{\{d\}} \\ j\sin\theta_{k,p}^{\{d\}} & -j\cos\theta_{k,p}^{\{d\}} \end{pmatrix} \in \mathbb{C}^{2\times 2},$$

and $j = \sqrt{-1}$. $\mathbf{W}_k^{\{d\}}, \mathbf{U}_k^{\{d\}} \in \mathbb{R}^{\frac{P}{2}\times\frac{P}{2}}$ are arbitrary real matrices and $\phi_p, \theta_{k,p}^{\{d\}} \in \mathbb{R}$ are arbitrary angle parameters. We adopt the initial matrix $\mathbf{E}_0(\mathbf{z})$ defined by

$$\mathbf{E}_0(\mathbf{z}) = \mathbf{V}_0 \mathbf{\Phi}_0^* \mathbf{E}_{\mathrm{DFT}}, \tag{11}$$

where $\mathbf{E}_{\mathrm{DFT}} \in \mathbb{C}^{M\times M}$ represents a matrix form of the 2-D discrete Fourier transform (DFT), $\mathbf{V}_0 \in \mathbb{R}^{P\times M}$ is an arbitrary left invertible matrix, and $\mathbf{\Phi_0} \in \mathbb{C}^{M\times M}$ is a unitary diagonal matrix which satisfies $\mathbf{E}_{\mathrm{DFT}} = \mathbf{\Phi}_0^2 \mathbf{E}_{\mathrm{DFT}}^* \mathbf{J}$, where $\mathbf{\Phi}_0$ always exists because $\mathbf{E}_{\mathrm{DFT}}$ has the LP property. ℂNSOLT is capable of being oversampled, overlapped, compact-supported, symmetric and nonseparable with complex-valued atomic images. If matrices $\{\mathbf{W}_k^{\{d\}}\}$ and $\{\mathbf{U}_k^{\{d\}}\}$ are orthogonal, then $\mathbf{E}(\mathbf{z})$ becomes PU.

3.3.1. No DC-Leakage Condition

If only one channel takes the piecewise DC component, the system is said to have no DC-leakage [7]. This property is important to construct a multiresolution analysis system. The condition is expressed by

$$\mathbf{E}(\mathbf{z}^{\mathbf{M}})\mathbf{d}_{\mathbf{M}}(\mathbf{z})\Big|_{\mathbf{z}=1} = \mathbf{E}(\mathbf{1})\mathbf{d}_{\mathbf{M}}(\mathbf{1}) = (c,\ 0, \cdots,\ 0)^T \tag{12}$$

where c is an arbitrary nonzero constant [7]. Then, no-DC-leakage condition for Type-I ℂNSOLT is given by

$$\begin{pmatrix} \left(\prod_{k=1}^{K_{\mathrm{v}}} \mathbf{W}_k^{\{\mathrm{v}\}}\right)\left(\prod_{k=1}^{K_{\mathrm{h}}} \mathbf{W}_k^{\{\mathrm{h}\}}\right) & \mathbf{O} \\ \mathbf{O} & \mathbf{I} \end{pmatrix} \mathbf{V}_0 = \begin{pmatrix} 1 & \mathbf{o}^T \\ \mathbf{o} & \bar{\mathbf{V}} \end{pmatrix}, \tag{13}$$

where $\bar{\mathbf{V}} \in \mathbb{R}^{(P-1)\times M}$ is an arbitrary left invertible matrix.

3.3.2. Dictionary Learning of Paraunitary ℂNSOLT

A PU ℂNSOLT synthesis system, i.e., $\mathbf{R}(\mathbf{z})$ obtained by paraconjugation of PU ℂNSOLT analysis one as in (7), yields a complex-valued tight frame dictionary and can be designed through the example-based approach similar to the ℝNSOLT case [7, 10]. The design problem is formulated as

$$\left\{\hat{\mathbf{D}}, \{\hat{\mathbf{y}}_i\}\right\} = \arg\min_{\mathbf{D},\mathbf{y}} \frac{1}{S} \sum_{i=0}^{S-1} \|\mathbf{x}_i - \mathbf{D}\mathbf{y}_i\|_2^2 \text{ s.t. } \|\mathbf{y}_i\|_0 \le K, \tag{14}$$

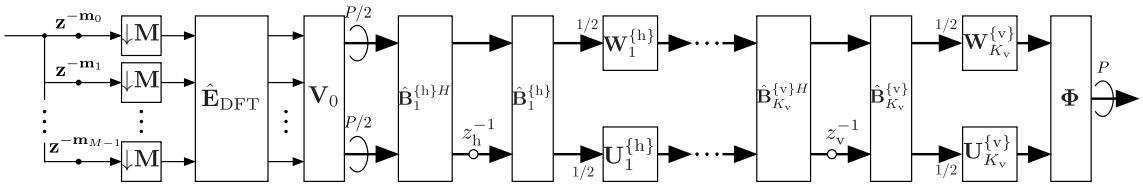

Fig. 2. Lattice structure of analysis bank of 2-D Type-I complex nonseparable OS lapped transform (ℂNSOLT)

where $\{\mathbf{x}_i\}$ is a set of training images and S is the cardinality. The design process consists of *sparse approximation* and *dictionary update*. The two stages are alternatively iterated to obtain an optimal dictionary.

- *Sparse approximation stage* searches coefficient vector $\mathbf{y}$ which minimize the approximation errors for training image $\mathbf{x}_i$ under K-sparse constraint with a fixed dictionary $\hat{\mathbf{D}}$. The optimization problem is formulated as

$$\hat{\mathbf{y}}_i = \arg\min_{\mathbf{y}} \|\mathbf{x}_i - \mathbf{D}\mathbf{y}\|_2^2 \text{ s.t. } \|\mathbf{y}_i\|_0 \leq K. \tag{15}$$

- *Dictionary update stage* searches a dictionary $\mathbf{D}$ which minimizes the approximation error for training images $\{\mathbf{x}_i\}$ with fixed coefficient vectors $\{\hat{\mathbf{y}}_i\}$. A PU ℂNSOLT is designed by controlling angle parameters $\boldsymbol{\phi} = (\phi_0, \phi_1, \cdots, \phi_{P-1})$ and $\boldsymbol{\theta} = (\theta_0, \theta_1, \cdots, \theta_{J-1})$, and sign parameter $\mathbf{s} = (s_0, s_1, \cdots, s_{I-1})$, where $\boldsymbol{\theta}$ and $\mathbf{s}$ are parameters for Givens factorization of orthonormal matrices. I and J are the numbers of the elements of $\mathbf{s}$ and $\boldsymbol{\theta}$, respectively. The optimization problem is formulated as

$$\hat{\boldsymbol{\Theta}} = \arg\min_{\boldsymbol{\Theta}} \frac{1}{S} \sum_{i=0}^{S-1} \|\mathbf{x}_i - \mathbf{D}_{\boldsymbol{\Theta}} \hat{\mathbf{y}}_i\|_2^2, \tag{16}$$

  where $\mathbf{D}_{\boldsymbol{\Theta}}$ is a ℂNSOLT dictionary determined by parameters $\boldsymbol{\Theta} = \{\boldsymbol{\phi}, \boldsymbol{\theta}, \mathbf{s}\}$. The updated dictionary $\hat{\mathbf{D}} = \hat{\mathbf{D}}_{\hat{\boldsymbol{\Theta}}}$ is used in the next sparse coding stage.

4. PERFORMANCE EVALUATION

To verify the significance of the proposed structure, let us show design examples and evaluate their sparse approximation performances by using IHT.

4.1. Design Examples

Figs. 3 and 4 show designed atomic images of ℝNSOLT and ℂNSOLT, respectively. The common specification is given below.

- Downsampling factor: $\mathbf{M} = \mathrm{diag}(M_\mathrm{v}, M_\mathrm{h}) = \mathrm{diag}(2, 2)$
- #Channels: $P = 6$
- Polyphase order: $N_\mathrm{v} = N_\mathrm{h} = 4$
- No-DC-leakage condition: Satisfied
- #Tree Levels: $\tau = 4$
- Redundancy: $R < \frac{P-1}{M-1} = \frac{5}{3}$
- Boundary operation: Periodic extension
- Sparse approximation: IHT
- #Traning images: $S = 1$ (Fig. 5)

Fig. 3. Atomic images of ℝNSOLT

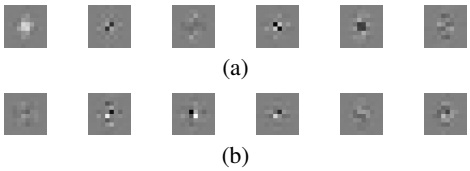

Fig. 4. Atomic images of ℂNSOLT. (a) real part. (b) imaginary part.

4.2. Sparse Approximation

We performed sparse approximation of complex-valued image. Fig. 5 shows the original, a millimeter wave radar image of size $2,992 \times 320$ pixels. The results of IHT with $K = 12.5\%$ are shown in Fig. 6. ℂNSOLT shows a superior performance to ℝNSOLT.

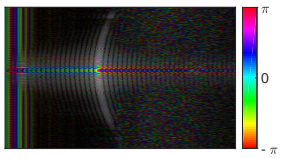

Fig. 5. Original image of size $2,992 \times 320$[pixels], where the intensity and hue show the magnitude and phase characteristics, respectively.

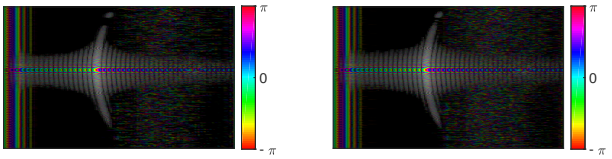

Fig. 6. Sparse approximation results with 2-D NSOLT dictionaries through IHT. (a) ℝNSOLT, MSE $= 2.36 \times 10^{-5}$, (b) ℂNSOLT, MSE $= 1.59 \times 10^{-5}$.

5. CONCLUSION

In this work, we generalized the theory of ℝNSOLT in [7] to the complex-valued case. The effectiveness of the proposed method was examined for a millimeter wave radar image by sparse approximation with IHT. As future works, we are interested in applying ℂNSOLTs to complex-valued image restoration.

6. REFERENCES

[1] Z. Cvetković and M. Vetterli, "Oversampled filter banks," *IEEE Transactions on Signal Processing*, vol. 46, no. 5, pp. 1245–1255, May 1998.

[2] L. Zhao, L. Wang, L. Yang, A. M. Zoubir, and G. Bi, "The race to improve radar imagery: An overview of recent progress in statistical sparsity-based techniques," *IEEE Signal Processing Magazine*, vol. 33, no. 6, pp. 85–102, Nov 2016.

[3] Y. C. Eldar and G. Kutyniok, *Compressed Sensing: Theory and Applications*, Compressed Sensing: Theory and Applications. Cambridge University Press, 2012.

[4] Michael Elad, *Sparse and Redundant Representations: From Theory to Applications in Signal and Image Processing*, Springer Publishing Company, Incorporated, 1st edition, 2010.

[5] I. Rish and G. Grabarnik, *Sparse Modeling: Theory, Algorithms, and Applications*, Chapman & Hall. Taylor & Francis, 2014.

[6] B. Wohlberg, "Boundary handling for convolutional sparse representations," in *2016 IEEE International Conference on Image Processing (ICIP)*, Sept 2016, pp. 1833–1837.

[7] S. Muramatsu, K. Furuya, and N. Yuki, "Multidimensional nonseparable oversampled lapped transforms: Theory and design," *IEEE Transactions on Signal Processing*, vol. 65, no. 5, pp. 1251–1264, March 2017.

[8] K. Seino, K. Furuya, and S. Muramatsu, "Transposition-based architecture of 2-D non-separable oversampled lapped transforms," in *Signal and Information Processing Association Annual Summit and Conference (APSIPA), 2014 Asia-Pacific*, Dec 2014, pp. 1–6.

[9] S. Muramatsu, "Structured dictionary learning with 2-D nonseparable oversampled lapped transform," in *2014 IEEE International Conference on Acoustics, Speech and Signal Processing (ICASSP)*, May 2014, pp. 2624–2628.

[10] S. Muramatsu, M. Ishii, and Z. Chen, "Efficient parameter optimization for example-based design of nonseparable oversampled lapped transform," in *2016 IEEE International Conference on Image Processing (ICIP)*, Sept 2016, pp. 3618–3622.

[11] T. Adali and P. J. Schreier, "Optimization and estimation of complex-valued signals: Theory and applications in filtering and blind source separation," *IEEE Signal Processing Magazine*, vol. 31, no. 5, pp. 112–128, Sept 2014.

[12] Peter J Schreier and Louis L Scharf, *Statistical signal processing of complex-valued data: the theory of improper and noncircular signals*, Cambridge University Press, 2010.

[13] P. P. Vaidyanathan, *Multirate Systems and Filter Banks*, Prentice-Hall signal processing series. Prentice Hall, 1993.

[14] I. W. Selesnick, R. G. Baraniuk, and N. C. Kingsbury, "The dual-tree complex wavelet transform," *IEEE Signal Processing Magazine*, vol. 22, no. 6, pp. 123–151, Nov 2005.

[15] T. Blumensath and M. E. Davies, "Normalized iterative hard thresholding: Guaranteed stability and performance," *IEEE Journal of Selected Topics in Signal Processing*, vol. 4, no. 2, pp. 298–309, April 2010.

[16] X. Q. Gao, T. Q. Nguyen, and G. Strang, "Theory and lattice structure of complex paraunitary filterbanks with filters of (hermitian-)symmetry/antisymmetry properties," *IEEE Transactions on Signal Processing*, vol. 49, no. 5, pp. 1028–1043, May 2001.